25th ABCM International Congress of Mechanical Engineering
October 20-25, 2019, Uberlândia, MG, Brazil

COB-2019-0585
ANALYSIS OF AN ASYMMETRIC PARALLEL MANIPULATOR FOR DETERMINATION OF PROMISING KINEMATIC AND DYNAMIC PARAMETERS

Rodrigo Magalhães Cruz Alves Silva
Department of Mechatronics and Mechanical Systems Engineering, Escola Politécnica, University of Sao Paulo, Brazil.
e-mail: rodrigomagalhaes@usp.br
Fernando Malvezzi
Department of Mechanical Engineering, Maua Institute of Technology, Brazil.
email: fernando.malvezzi@maua.br
Tarcísio Antônio Hess Coelho
Department of Mechatronics and Mechanical Systems Engineering, Escola Politécnica, University of Sao Paulo, Brazil.
e-mails: tarchess@usp.br

Abstract. *This work deals with the analysis of the model of an asymmetric parallel manipulator investigating parameters for improving the performance in terms of stiffness and natural frequencies throughout the workspace, seeking conditions in which the real and ideal properties are close, and thus accurately predict its behavior. The mapping of the stiffness and natural frequencies of the manipulator within its workspace is obtained using the lumped parameters method, assuming the existence of virtual actuators as an alternative to consider the flexibility effects of the manipulator links. In addition, the passive chain effect will also be taken into account to maintain the end effector orientation in relation to the loading. When these effects are considered, the Jacobian matrix associated to the space of the actuators undergoes a change in size and additional considerations are required to determine the stiffness matrix for a configuration of the manipulator. This allows concluding that the use of the lumped parameters associated with the inclusion of virtual actuators allows a simpler and more efficient formulation of deflection and frequencies of the end effector, thus representing a better alternative for analyzing parallel manipulators, providing results that will serve as the background for the parametric synthesis of the mechanism.*

Keywords: *Parallel Manipulators, Stiffness, Natural Frequencies, Mapping, Lumped Parameters Method.*

1. INTRODUCTION

Currently, most industrial robots are based on a category defined as open chain, i.e. the links and actuators are arranged in series, one after another one, with a free end effector working as a manipulator or a tool. However, for the last three decades researches have been developing closed-loop mechanisms with the end effector connected to the base by at least two kinematic chains acting simultaneously (Craig, 2005, Bonev, 2019).

This new architecture is considered promising due to some potential advantages compared to serial mechanisms, such as stiffness, high load capacity, accuracy and fast dynamic response (Majou et al, 2007). On the other hand, this architecture, called parallel mechanism, also showed some disadvantages, namely, an existence of a relatively complex workspace, a non-linearity between rates of the actuators and the end effector, represented by the Jacobian matrix. This non-linearity may be a serious problem, especially in machining operations, where a constant motion is necessary during the process. Some articles were proposed to overcome these disadvantages. Chablat and Wenger (2003) developed a parallel mechanism called orthoglide in which the workspace is cubic with regular isotropic characteristics. The regularity and the isotropy were obtained by synthesizing a mechanism with three equal kinematic chains, which generated a symmetrical parallel kinematic mechanism. Cammarata (2016) sought a unified formulation of space manipulators using condensation techniques and partitioned matrices. Liu et al (2017) also looked for ways of obtaining the stiffness matrix of parallel manipulators by applying a semi-analytic hierarchical approach at the level of joints and links. Regarding to dynamic analysis of flexible parallel mechanism, many methodologies have been applied, such as lumped parameters method (Liang et al, 2017, Rezaei et al, 2012), assumed mode method (Chen, 2001) and finite elements approach (Wang and Mills, 2005, Zhang, 2015).

While there are only few works that approach asymmetric architectures, most of the proposed parallel robot architectures present symmetric kinematic chains. Although many researchers prefer isotropic structure, there are some applications for parallel mechanism in which the speed and stiffness requirements do not need to be the same in all the directions.

Parametric synthesis is another meaningful topic to be achieved in the mechanism design. It consists in a process of searching the parameters of the mechanism, whether kinematic or dynamic, according to chosen criterion. Among the proposed methods, property mapping, sensitivity analysis and optimization are remarked. Property mapping refers to the graphical representation of the distribution of some properties into the workspace, such as stiffness and natural frequency, useful to develop the design of a mechanism (Long et al, 2018, Silva and Hess-Coelho, 2019). The sensitivity analysis evaluates the influence of a variation of some parameters on the mechanism performance (Zi et al, 2014). Optimization, in turn, is the problem of finding the optimal parameters of the mechanism which maximize or minimize a function associated to the performance of the mechanism (Haftka, 1992). For instance, the function may represent mathematically the end effector location accuracy or the size of workspace (Zhao, 2013).

This paper establishes the mapping of the stiffness and natural frequencies of the manipulator within its workspace by applying the lumped parameters method. After the *2RSS + PPaP* mechanism has been introduced, the inverse kinematics of the plane version of the mechanism will be performed in order to determine its workspace. Then, using the method of the lumped parameters, a model with springs representing the various sources of flexibility of the mechanism links will be created, including the passive chain. The stiffness matrix of the mechanism, which relates forces acting on the end effector and their respective displacements, will be developed. The inertia matrix of the mechanism in the end effector space will be also determined by applying the Jacobian matrices of the mechanism links.

Finally, simulations of the mechanism end effector displacements under static loads, and the mapping of the first natural frequency along the mechanism workspace will be performed. A comparison between the model, that considers the sources of flexibility of the passive chain, and the another one that does not consider its effects, enables verification of the passive chain relevance in some features of the mechanism.

2. METHODOLOGY

In Fig. 1, it is shown the manipulator that will be object of study. It has three active limbs that connect a fixed base to an end effector. In its conception the alternative procedure of synthesis of the type proposed by Hess-Coelho (2007) is used, in which the degrees of freedom of the end effector are imposed by one of the members (in this case the central limb). Using the *R*, *P* and *S* notation to indicate the rotation, prismatic and spherical joints, respectively, and the symbol Pa for a subchain of the articulated parallelogram type, its two lateral members may be described as of the *RSS* type while its central member of the *PPaP* type. Underlined letters indicate active joints. Thus, the architecture of the mechanism is the type *2RSS + PPaP*.

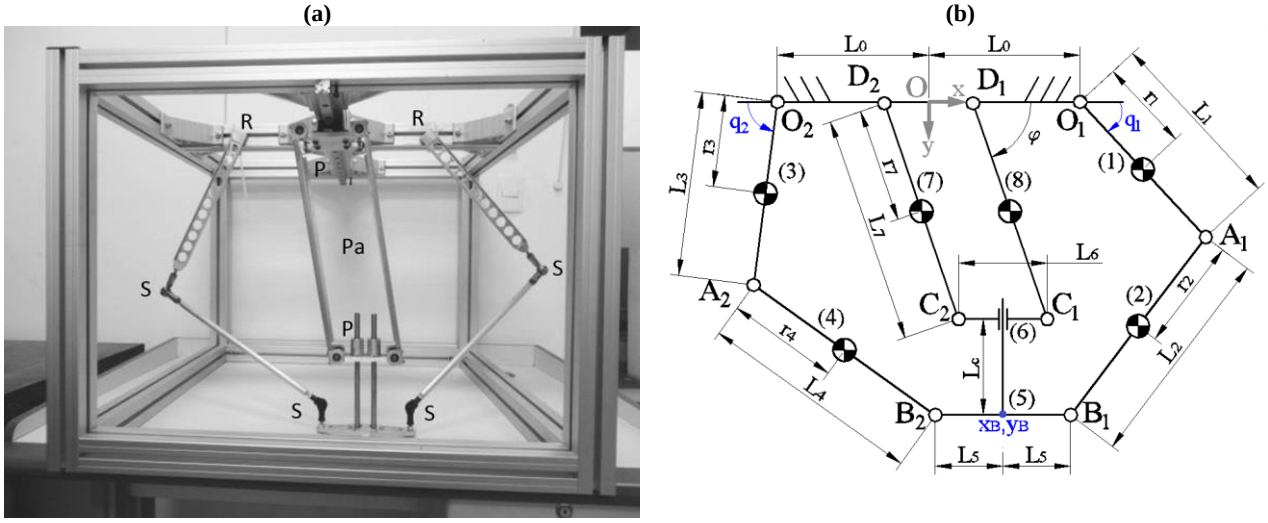

Figure 1 – (a) Manipulator *2RSS + PPaP* with the types of joints indicated and (b) schematic diagram with dimensions and the numbering of links (indicated in parentheses).

Although it has planes of geometric symmetry, the mechanism is asymmetrical from the viewpoint of the topology, since the limbs do not have the same sequence of joints (Tsai, 1999). The development of all stages of the design of this manipulator was based on several aspects of commercial parallel architecture manipulator robots, specifically the FlexPicker IRB 360-3 / 1130 (ABB Robotics, 2013) and the Adept Quattro s650H (Adept Technology, 2010).

2.1 Mechanism workspace and inverse kinematics

In order to determine the mechanism workspace, several positions are assigned to the mechanism end effector and inverse kinematics are applied to determine the configuration of the actuators to generate such a position. Although the

mechanism originally has 3 degrees of freedom, all development was done in the *XY* plane indicated in Fig. 1, thus the prismatic joint of the central chain was not considered, and this becomes a passive chain in the plane model. To perform the inverse kinematics, it is necessary to determine the closed-loop equations of the mechanism. For the *RSS* limb of the right side of the kinematic structure, once the lengths of the lower links in the limbs *RSS* are constant, then:

$$f_{1r}(q_1, q_2, x_B, y_B) = (-L_1 \cos q_1 - L_0 + x_B + L_5)^2 + (-L_1 \sin q_1 + y_B)^2 - {L_2}^2 = 0 \quad (1)$$

Similarly, for the *RSS* member on the left side, we obtain

$$f_{2r}(q_1, q_2, x_B, y_B) = (L_3 \cos q_2 + L_0 + x_B - L_5)^2 + (-L_3 \sin q_2 + y_B)^2 - {L_4}^2 = 0 \quad (2)$$

All terms in Eqs. (1) and (2) are shown in Fig. 1. It should be noted that these closed-loop equations refer to the rigid body kinematics of the mechanism. These same equations will be slightly modified in Section 2.2 to consider the flexibility effect of the passive chain. For the inverse kinematics, the terms $\sin q_1$, $\sin q_2$, $\cos q_1$ and $\cos q_2$ of Eq. (1) and Eq. (2) can be grouped together, and using trigonometric identities, the set of values of q_1 and q_2 were determined (Silva and Hess-Coelho, 2019). For all further development, the sets of solutions chosen for q_1 and q_2 are restricted to the values comprised between *0 rad* and *π/2 rad*. Thus, it is ensured that the configurations of the chains $O_1A_1B_1$ and $O_2A_2B_2$ in Fig. 1 will be positioned outwardly avoiding possible interference between those limbs and the articulated parallelogram. For those cases in which the solution is possible, that is, without complex solutions, presence of singularities of the workspace limit or the length of the end effector's cursor L_c, a sketch of the workspace of the mechanism is determined in Fig. 2.

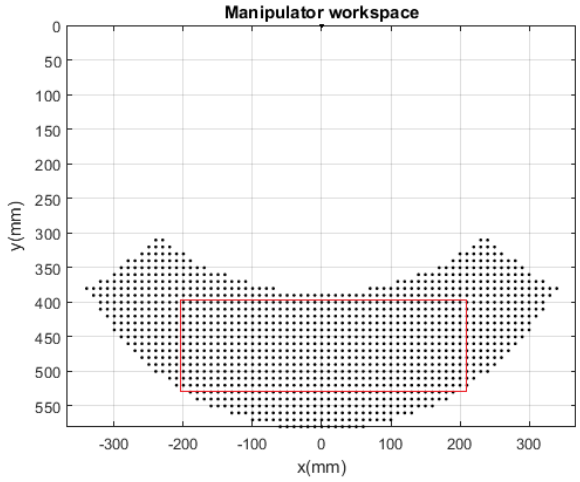

Figure 2 – Workspace of the manipulator *2RSS+PPaP* and area for mapping of stiffness and natural frequencies indicated by the rectangle (Silva and Hess-Coelho, 2019).

2.2 Formulation of the stiffness matrix

In the present work, the lumped parameters method (Gosselin, 1990) will be applied considering the stiffness of the mechanism links, in order to obtain the mapping of the stiffness throughout the workspace of the mechanism. So, it will be possible to investigate as the various parameters of the manipulator affect the mapping of stiffness and natural frequency. The analysis was linear, not taking into account, therefore, effects of geometric nonlinearities, of the material, buckling, etc.

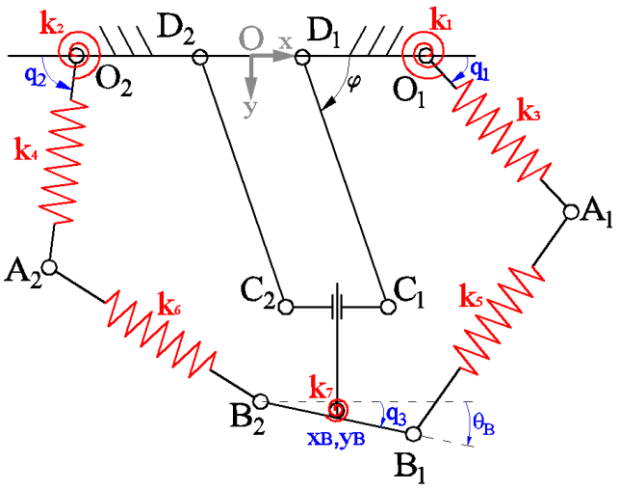

Figure 3 – Scheme of the mechanism using spring elements to consider the various sources of elasticity of the links.

For the parallel kinematics manipulator, the stiffness matrix in the end effector space $\boldsymbol{K_x}$, considering as sources of flexibility only the transmission in the actuators of the mechanism, is given by (Zhang, 2009):

$$\boldsymbol{K_x} = \boldsymbol{J'^{-T} K_q J'^{-1}} \tag{3}$$

Where $\boldsymbol{J'}$ is the Jacobian matrix relating the rates of the actuators and the end effector in the Cartesian space and $\boldsymbol{K_q}$ is a diagonal stiffness matrix relating the forces and displacements in the actuators. The matrix $\boldsymbol{J'}$ is defined as

$$\boldsymbol{J'} = \boldsymbol{J_x^{-1} J_{qext}} \tag{4}$$

The matrices $\boldsymbol{J_{qext}}$ and $\boldsymbol{J_x}$ are given by

$$\boldsymbol{J_x} = \frac{\partial \boldsymbol{f}}{\partial \boldsymbol{x}} \tag{5}$$

$$\boldsymbol{J_{qext}} = -\frac{\partial \boldsymbol{f}}{\partial \boldsymbol{q}} \tag{6}$$

Where $\boldsymbol{f}$ is a vector of dimension equal to the mobility of the mechanism, implicitly relating the vectors $\boldsymbol{x}$ and $\boldsymbol{q}$, the kinematic constraint equations of the chains.

In order to take into account other sources of flexibility of the manipulator, such as the links, it is assumed that there are virtual actuators acting on the degrees of freedom, associated with the displacements of the links that will be considered as a source of flexibility. In this case, the problem becomes the analysis of a mechanism with kinematic redundancy (Fontes and da Silva, 2016). In the case of the manipulator under study in Fig. 3, it considers the existence of virtual linear actuators in the four links (O_1A_1, O_2A_2, A_1B_1 e A_2B_2), two rotary actuators in the joints of the manipulator base (points O_1 e O_2), and a rotary actuator at the end of the passive chain defining an inclination of the end effector, which stiffness values are imposed by the values obtained by the stiffness of the real links, for the associated relative displacements. In the case of rotary actuators, it is still possible to consider flexibility, due to the actuators and the links simultaneously, simply by considering an association of torsion springs in series.

In considering the existence of these virtual actuators, the matrix $\boldsymbol{J_{qext}}$ becomes rectangular, making it impossible to invert $\boldsymbol{J'}$ in the definition of the stiffness matrix in Eq. (3). To solve this problem, the properties of the inverse of the matrix product are applied (Zhang and Gosselin, 2002), resulting in

$$\boldsymbol{K_x} = \left(\boldsymbol{J' K_q}^{-1} \boldsymbol{J'^T}\right)^{-1} \tag{7}$$

For modeling the stiffness of the passive chain, a new constraint equation f_3 was introduced relating the end effector angle θ_B, and the angular displacement of the spring k_7, q_3, as shown in Fig. 3. The closed-loop equations of the two <u>*RSS*</u> limbs of the mechanism indicated in Eqs. (1) and (2) must also be modified to consider the rotation of the end effector.

$$f_1(q_1, q_2, x_B, y_B, \theta_B) = (-L_1 \cos q_1 - L_0 + x_B + L_5 \cos \theta_B)^2 + (-L_1 \sin q_1 + y_B + L_5 \sin \theta_B)^2 - {L_2}^2 = 0 \tag{8}$$

$$f_2(q_1, q_2, x_B, y_B, \theta_B) = (L_3 \cos q_2 + L_0 + x_B - L_5 \cos \theta_B)^2 + (-L_3 \sin q_2 + y_B - L_5 \sin \theta_B)^2 - {L_4}^2 = 0 \quad (9)$$

$$f_3(q_3, \theta_B) = \theta_B - q_3 = 0 \quad (10)$$

Determining the partial derivatives to obtain the Jacobian matrices $\boldsymbol{J_{qext}}$ and $\boldsymbol{J_x}$ and considering the virtual actuators, we obtain

$$\boldsymbol{J_{qext}} = -\begin{bmatrix} \frac{\partial f_1}{\partial q_1} & \frac{\partial f_1}{\partial q_2} & \frac{\partial f_1}{\partial L_1} & \frac{\partial f_1}{\partial L_3} & \frac{\partial f_1}{\partial L_2} & \frac{\partial f_1}{\partial L_4} & \frac{\partial f_1}{\partial q_3} \\ \frac{\partial f_2}{\partial q_1} & \frac{\partial f_2}{\partial q_2} & \frac{\partial f_2}{\partial L_1} & \frac{\partial f_2}{\partial L_3} & \frac{\partial f_2}{\partial L_2} & \frac{\partial f_2}{\partial L_4} & \frac{\partial f_2}{\partial q_3} \\ \frac{\partial f_3}{\partial q_1} & \frac{\partial f_3}{\partial q_2} & \frac{\partial f_3}{\partial L_1} & \frac{\partial f_3}{\partial L_3} & \frac{\partial f_3}{\partial L_2} & \frac{\partial f_3}{\partial L_4} & \frac{\partial f_3}{\partial q_3} \end{bmatrix} = \begin{bmatrix} J_{qext11} & 0 & J_{qext13} & 0 & 2L_2 & 0 & 0 \\ 0 & J_{qext22} & 0 & J_{qext24} & 0 & 2L_4 & 0 \\ 0 & 0 & 0 & 0 & 0 & 0 & 1 \end{bmatrix} \quad (11)$$

$$\boldsymbol{J_x} = \begin{bmatrix} \frac{\partial f_1}{\partial x_B} & \frac{\partial f_1}{\partial y_B} & \frac{\partial f_1}{\partial \theta_B} \\ \frac{\partial f_2}{\partial x_B} & \frac{\partial f_2}{\partial y_B} & \frac{\partial f_2}{\partial \theta_B} \\ \frac{\partial f_3}{\partial x_B} & \frac{\partial f_3}{\partial y_B} & \frac{\partial f_3}{\partial \theta_B} \end{bmatrix} = \begin{bmatrix} 2(-L_0 + x_B - L_1 cosq_1 + L_5 cos\theta_B) & 2\,(y_B - L_1 sinq_1 + L_5 sin\theta_B) & J_{x13} \\ 2(L_0 + x_B + L_3 cosq_2 - L_5 cos\theta_B) & 2\,(y_B - L_3 sinq_2 - L_5 sin\theta_B) & J_{x23} \\ 0 & 0 & 1 \end{bmatrix} \quad (12)$$

Where

$$J_{qext11} = 2L_1 cosq_1(y_B - L_1 sinq_1 + L_5 sin\theta_B) - 2L_1 sinq_1(-L_0 + x_B - L_1 cosq_1 + L_5 cos\theta_B) \quad (13)$$

$$J_{qext22} = 2L_3(L_0 + x_B + L_3 cosq_2 - L_5 cos\theta_B) sinq_2 + 2L_3 cosq_2(y_B - L_3 sinq_2 - L_5 sin\theta_B) \quad (14)$$

$$J_{qext13} = 2cosq_1(-L_0 + x_B - L_1 cosq_1 + L_5 cos\theta_B) + 2sinq_1(y_B - L_1 sinq_1 + L_5 sin\theta_B) \quad (15)$$

$$J_{qext24} = 2sinq_2(y_B - L_3 sinq_2 - L_5 sin\theta_B) - 2cosq_2(L_0 + x_B + L_3 cosq_2 - L_5 cos\theta_B) \quad (16)$$

$$J_{x13} = 2\,L_5 cos\theta_B(y_B - L_1 sinq_1 + L_5 sin\theta_B) - 2L_5 sin\theta_B(-L_0 + x_B - L_1 cosq_1 + L_5 cos\theta_B) \quad (17)$$

$$J_{x23} = 2L_5 sin\theta_B(L_0 + x_B + L_3 cosq_2 - L_5 cos\theta_B) - 2L_5 cos\theta_B(y_B - L_3 sinq_2 - L_5 sin\theta_B) \quad (18)$$

The stiffness matrix in the actuator space $\boldsymbol{K_q}$ is defined by

$$\boldsymbol{K_q} = \begin{bmatrix} k_1 & 0 & 0 & 0 & 0 & 0 & 0 \\ 0 & k_2 & 0 & 0 & 0 & 0 & 0 \\ 0 & 0 & k_3 & 0 & 0 & 0 & 0 \\ 0 & 0 & 0 & k_4 & 0 & 0 & 0 \\ 0 & 0 & 0 & 0 & k_5 & 0 & 0 \\ 0 & 0 & 0 & 0 & 0 & k_6 & 0 \\ 0 & 0 & 0 & 0 & 0 & 0 & k_7 \end{bmatrix} = \begin{bmatrix} \frac{3EI_{A1}}{L_1} & 0 & 0 & 0 & 0 & 0 & 0 \\ 0 & \frac{3EI_{A3}}{L_3} & 0 & 0 & 0 & 0 & 0 \\ 0 & 0 & \frac{EA_1}{L_1} & 0 & 0 & 0 & 0 \\ 0 & 0 & 0 & \frac{EA_3}{L_3} & 0 & 0 & 0 \\ 0 & 0 & 0 & 0 & \frac{EA_2}{L_2} & 0 & 0 \\ 0 & 0 & 0 & 0 & 0 & \frac{EA_4}{L_4} & 0 \\ 0 & 0 & 0 & 0 & 0 & 0 & k_7 \end{bmatrix} \quad (19)$$

The element k_7 represents the stiffness of the passive chain and is given by

$$k_7 = \left(\frac{1}{2L_6 \tan^2 \varphi A_6 E} + \frac{L_7}{4L_6^2 \sin^2 \varphi A_7 E} + \frac{L_8}{4L_6^2 \sin^2 \varphi A_8 E} + \frac{L_6^5}{6EI_{A6}}\right)^{-1} \quad (20)$$

The elements of the main diagonal k_i (i=1…7); of Eq. (19), are springs with the value of stiffness, axial and to the bending, equal to the represented links, A_i (i=1…8) is the cross sectional area of the links and I_{A1}, I_{A3} and I_{A6} are the second moment of area of the links 1, 3 and 6, respectively. The description of the stiffness of these virtual actuators was fully described in (Gosselin and Zhang, 2002).

2.3 Formulation of the inertia matrix

The kinetic energy of the mechanism T is given by

$$T = \frac{1}{2}\sum_{i=1}^{n_e} T_i = \frac{1}{2}\sum_{i=1}^{n_e} \boldsymbol{V_i^T M_i V_i} \tag{21}$$

Where n_e is the number of links of the mechanism. Working with the kinetic energy of only one link of the mechanism T_i, one can obtain

$$T_i = \boldsymbol{V_i^T M_i V_i} = \begin{bmatrix} v_{xi} & v_{yi} & v_{zi} & \omega_{xi} & \omega_{yi} & \omega_{zi} \end{bmatrix} \begin{bmatrix} m_i & 0 & 0 & 0 & 0 & 0 \\ 0 & m_i & 0 & 0 & 0 & 0 \\ 0 & 0 & m_i & 0 & 0 & 0 \\ 0 & 0 & 0 & I_{xi} & 0 & 0 \\ 0 & 0 & 0 & 0 & I_{yi} & 0 \\ 0 & 0 & 0 & 0 & 0 & I_{zi} \end{bmatrix} \begin{bmatrix} v_{xi} \\ v_{yi} \\ v_{zi} \\ \omega_{xi} \\ \omega_{yi} \\ \omega_{zi} \end{bmatrix} \tag{22}$$

Where m_i is the mass of the link i and $I_{xi},\ I_{yi},\ I_{zi}$ are the principal moments of inertia of the link i. Expressing the velocity components of the center of mass (v_{xi}, v_{yi}, v_{zi}) and angular ($\omega_{xi}, \omega_{yi}, \omega_{zi}$) in terms of the generalized velocities $\dot{\boldsymbol{q}}$, one obtain

$$\boldsymbol{V_i} = \begin{bmatrix} v_{xi} & v_{yi} & v_{zi} & \omega_{xi} & \omega_{yi} & \omega_{zi} \end{bmatrix}^T = \boldsymbol{C_i \dot{q}} \tag{23}$$

The matrix $\boldsymbol{C_i}$ is defined as the jacobian matrix of the link i, that is, the matrix that relates the velocity components of the center of mass and angular with the generalized velocities. Substituting Eq. (23) in Eq. (22), we obtain

$$T_i = (\boldsymbol{C_i \dot{q}})^T \boldsymbol{M_i} (\boldsymbol{C_i \dot{q}}) \tag{24}$$

Returning to the total kinetic energy and applying a property of the matrix product $\boldsymbol{(AB)^T = B^T A^T}$, one can obtain

$$T = \frac{1}{2}\sum_{i=1}^{n_e} \boldsymbol{\dot{q}^T (C_i^T M_i C_i) \dot{q}} = \frac{1}{2}\sum_{i=1}^{n_e} \boldsymbol{\dot{q}^T M_{qi} \dot{q}} \tag{25}$$

Where $\boldsymbol{M_{qi}}$ is the inertia matrix of the i link in the actuator space (Craig, 2005). Thus, the inertia matrix of the mechanism $\boldsymbol{M_q}$ is

$$\boldsymbol{M_q} = \sum_{i=1}^{n_e} \boldsymbol{M_{qi}} = \sum_{i=1}^{n_e} \boldsymbol{C_i^T M_i C_i} \tag{26}$$

Applying the conventional definition for the Jacobian matrix of parallel kinematic mechanisms $\boldsymbol{J}$, now relating the end effector velocities ($\dot{x}_B, \dot{y}_B, \dot{\theta}_B$) and the velocities of the actuators ($\dot{q}_1, \dot{q}_2, \dot{q}_3$), one can obtain

$$\boldsymbol{\dot{q}} = \left(\boldsymbol{J_q^{-1} J_x}\right) \boldsymbol{\dot{x}} = \boldsymbol{J \dot{x}} \tag{27}$$

Substituting Eq. (27) into Eq. (25) and reapplying the property of the matrix product, we obtain

$$T = \frac{1}{2}\sum_{i=1}^{n_e} (\boldsymbol{J\dot{x}})^T (\boldsymbol{C_i^T M_i C_i})(\boldsymbol{J\dot{x}}) = \frac{1}{2}\sum_{i=1}^{n_e} \boldsymbol{\dot{x}^T (J^T C_i^T M_i C_i J) \dot{x}} = \frac{1}{2}\sum_{i=1}^{n_e} \boldsymbol{\dot{x}^T (M_{xi}) \dot{x}} \tag{28}$$

Where $\boldsymbol{M_{xi}}$ is defined as the inertia matrix of the link i of the mechanism in the end effector space. Thus, the inertia matrix of the mechanism in the end effector space $\boldsymbol{M_x}$ is

$$\boldsymbol{M_x} = \sum_{i=1}^{n_e} \boldsymbol{M_{xi}} = \sum_{i=1}^{n_e} \boldsymbol{J^T C_i^T M_i C_i J} = \sum_{i=1}^{n_e} \boldsymbol{C_{xi}^T M_i C_{xi}} \tag{29}$$

where

$$\boldsymbol{C_{xi}} = \boldsymbol{C_i J} \tag{30}$$

is the jacobian matrix of the link i in the end effector space, that is, the matrix that relates the velocities of the center of mass and angular of the link i with the velocities of the end effector $\dot{\boldsymbol{x}}$.

$$\boldsymbol{V_i} = \begin{bmatrix} v_{xi} & v_{yi} & v_{zi} & \omega_{xi} & \omega_{yi} & \omega_{zi} \end{bmatrix}^T = \boldsymbol{C_{xi} \dot{x}} \tag{31}$$

For the mechanism kinematics, the $\boldsymbol{C_{xi}}$ matrices of the links are described below

$$\boldsymbol{V_1} = \begin{bmatrix} v_{x1} \\ v_{y1} \\ \omega_{z1} \end{bmatrix} = \boldsymbol{C_{x1}}\dot{\boldsymbol{x}} = \begin{pmatrix} -J_{11}r_1\, sinq_1 & -J_{12}r_1\, sinq_1 & -J_{13}r_1\, sinq_1 \\ J_{11}r_1\, cosq_1 & J_{12}r_1\, cosq_1 & J_{13}r_1\, cosq_1 \\ J_{11} & J_{12} & J_{13} \end{pmatrix} \begin{bmatrix} \dot{x}_B \\ \dot{y}_B \\ \dot{\theta}_B \end{bmatrix} \tag{32}$$

$$\boldsymbol{V_2} = \begin{bmatrix} v_{x2} \\ v_{y2} \\ \omega_{z2} \end{bmatrix} = \boldsymbol{C_{x2}}\dot{\boldsymbol{x}} = \begin{pmatrix} \frac{r_2}{L_2} - \frac{J_{11}\,L_1(L_2-r_2)sin\ q_1}{L_2} & -\frac{J_{12}L_1(L_2-r_1)sinq_1}{L_2} & -\frac{J_{13}L_1(L_2-r_2)sinq_1}{L_2} - \frac{L_5r_2sin\theta_B}{L_2} \\ \frac{J_{11}L_1(L_2-r_2)\,cos\,q_1}{L_2} & \frac{r_2}{L_2} + \frac{J_{12}L_1(L_2-r_2)\,cos\,q_1}{L_2} & \frac{J_{13}L_1(L_2-r_2)\,cos\,q_1}{L_2} + \frac{L_5r_2\,cos\,\theta_B}{L_2} \\ \frac{1+J_{11}L_1\,sin\,q_1}{-y_B+L_1\,sin\,q_1-L_5sin\theta_B} & \frac{J_{12}L_1\,sin\,q_1}{-y_B+L_1\,sin\,q_1-L_5sin\theta_B} & \frac{J_{13}L_1\,sin\,q_1-L_5sin\theta_B}{-y_B+L_1\,sin\,q_1-L_5sin\theta_B} \end{pmatrix} \begin{bmatrix} \dot{x}_B \\ \dot{y}_B \\ \dot{\theta}_B \end{bmatrix} \tag{33}$$

$$\boldsymbol{V_3} = \begin{bmatrix} v_{x3} \\ v_{y3} \\ \omega_{z3} \end{bmatrix} = \boldsymbol{C_{x3}}\dot{\boldsymbol{x}} = \begin{pmatrix} J_{21}r_3\, sinq_2 & J_{22}r_3\, sinq_2 & J_{23}r_3\, sinq_2 \\ J_{21}r_3\, cosq_2 & J_{22}r_3\, cosq_2 & J_{23}r_3\, cosq_2 \\ -J_{21} & -J_{22} & -J_{23} \end{pmatrix} \begin{bmatrix} \dot{x}_B \\ \dot{y}_B \\ \dot{\theta}_B \end{bmatrix} \tag{34}$$

$$\boldsymbol{V_4} = \begin{bmatrix} v_{x4} \\ v_{y4} \\ \omega_{z4} \end{bmatrix} = \boldsymbol{C_{x4}}\dot{\boldsymbol{x}} = \begin{pmatrix} \frac{r_4}{L_4} + \frac{J_{21}\,L_3(L_4-r_4)sinq_2}{L_4} & \frac{J_{22}L_3(L_4-r_4)sinq_2}{L_4} & \frac{J_{23}L_3(L_4-r_4)sinq_2}{L_2} + \frac{L_5r_4sin\theta_B}{L_4} \\ \frac{J_{21}L_3(L_4-r_4)\,cos\,q_2}{L_4} & \frac{r_4}{L_4} + \frac{J_{22}L_3(L_4-r_4)\,cos\,q_2}{L_4} & \frac{J_{23}L_3(L_4-r_4)\,cos\,q_2}{L_4} - \frac{L_5r_4\,cos\,\theta_B}{L_4} \\ \frac{1-J_{21}L_3\,sin\,q_2}{-y_B+L_3\,sin\,q_2+L_5sin\theta_B} & -\frac{J_{22}L_3\,sin\,q_2}{-y_B+L_3\,sin\,q_2+L_5sin\theta_B} & \frac{L_5sin\theta_B-J_{23}L_3\mathrm{sin}q_2}{-y_B+L_3\,sin\,q_2+L_5\,\mathrm{sin}\,\theta_B} \end{pmatrix} \begin{bmatrix} \dot{x}_B \\ \dot{y}_B \\ \dot{\theta}_B \end{bmatrix} \tag{35}$$

$$\boldsymbol{V_5} = \begin{bmatrix} v_{x5} \\ v_{y5} \\ \omega_{z5} \end{bmatrix} = \boldsymbol{C_{x5}}\dot{\boldsymbol{x}} = \begin{pmatrix} 1 & 0 & 0 \\ 0 & 1 & 0 \\ 0 & 0 & 1 \end{pmatrix} \begin{bmatrix} \dot{x}_B \\ \dot{y}_B \\ \dot{\theta}_B \end{bmatrix} \tag{36}$$

$$\boldsymbol{V_6} = \begin{bmatrix} v_{x6} \\ v_{y6} \\ \omega_{z6} \end{bmatrix} = \boldsymbol{C_{x6}}\dot{\boldsymbol{x}} = \begin{pmatrix} 1 & 0 & 0 \\ -\frac{1}{tan\varphi} & 0 & 0 \\ 0 & 0 & 0 \end{pmatrix} \begin{bmatrix} \dot{x}_B \\ \dot{y}_B \\ \dot{\theta}_B \end{bmatrix} \tag{37}$$

$$\boldsymbol{V_7} = \begin{bmatrix} v_{x7} \\ v_{y7} \\ \omega_{z7} \end{bmatrix} = \boldsymbol{C_{x7}}\dot{\boldsymbol{x}} = \begin{pmatrix} \frac{r_7}{L_7} & 0 & 0 \\ -\frac{r_7}{L_7tan\varphi} & 0 & 0 \\ -\frac{1}{L_7sin\varphi} & 0 & 0 \end{pmatrix} \begin{bmatrix} \dot{x}_B \\ \dot{y}_B \\ \dot{\theta}_B \end{bmatrix} \tag{38}$$

$$\boldsymbol{V_8} = \begin{bmatrix} v_{x8} \\ v_{y8} \\ \omega_{z8} \end{bmatrix} = \boldsymbol{C_{x8}}\dot{\boldsymbol{x}} = \begin{pmatrix} \frac{r_7}{L_7} & 0 & 0 \\ -\frac{r_7}{L_7tan\varphi} & 0 & 0 \\ -\frac{1}{L_7sin\varphi} & 0 & 0 \end{pmatrix} \begin{bmatrix} \dot{x}_B \\ \dot{y}_B \\ \dot{\theta}_B \end{bmatrix} \tag{39}$$

Where J_{ij} (i, j = 1,2,3) are the elements of the conventional Jacobian matrix. Formulating the eigenvalue and eigenvector problem of the system for determination of the natural frequencies of the system, we obtain

$$(\boldsymbol{K_x} - \omega^2\boldsymbol{M_x})\boldsymbol{\phi} = \boldsymbol{0} \tag{40}$$

Where ω is the natural frequency of the mechanism and $\boldsymbol{\phi}$ is the associated eigenvector. It is important to note that frequencies and vibrate modes are associated with each mechanism configuration.

3. RESULTS

For the manipulator data provided in Tab. 1 a mapping of the end effector stiffness of the mechanism is obtained in Fig. 4, for the region of the mechanism workspace indicated in Fig. 2, assuming the application of a unitary force in the positive direction of y. Figure 5 shows the mapping of the first natural frequency of the mechanism. In order to compare, the same mappings were made without considering the passive chain, thus, assuming that the end effector will remain horizontal, the mechanism will have mobility 2, disregarding the spring k_7 and the parameters q_3 and θ_B in Fig. 3. It was assumed that the real actuators are blocked in each configuration and assuming that they do not present flexibility,

considering only the sources of flexibility of the mechanism links. It has also been assumed that the links have the mass and cross-sectional area uniform across the length. In the present study, a computer with an Intel® Core i5 - 36100M 2.30 GHz processor, 4 GB DDR3 memory, was used. All the numerical simulations to obtain the mappings were performed using routines in MatLab®.

Table 1 – Parameters for the manipulator links

Dimensions (mm)	Mass (kg)	Area links (mm^2)	Second moment of area (mm^4)	Young's modulus (GPa)
$L_0 = 180$				
$L_1 = L_3 = 350$	$m_1 = m_3 = 0.321$	$A_1 = A_3 = 220.0$	$I_{A1} = I_{A3} = 1.47 \cdot 10^4$	
$L_2 = L_4 = 422$	$m_2 = m_4 = 0.213$	$A_2 = A_4 = 160.6$	$I_{A2} = I_{A4} = 2.05 \cdot 10^3$	69
$L_5 = 160$	$m_5 = 0.650$			
$L_6 = 100$	$m_6 = 0.143$		$I_{A6} = 1.47 \cdot 10^4$	
$L_7 = L_8 = 385$	$m_7 = m_8 = 0.134$	$A_7 = A_8 = 160.6$		

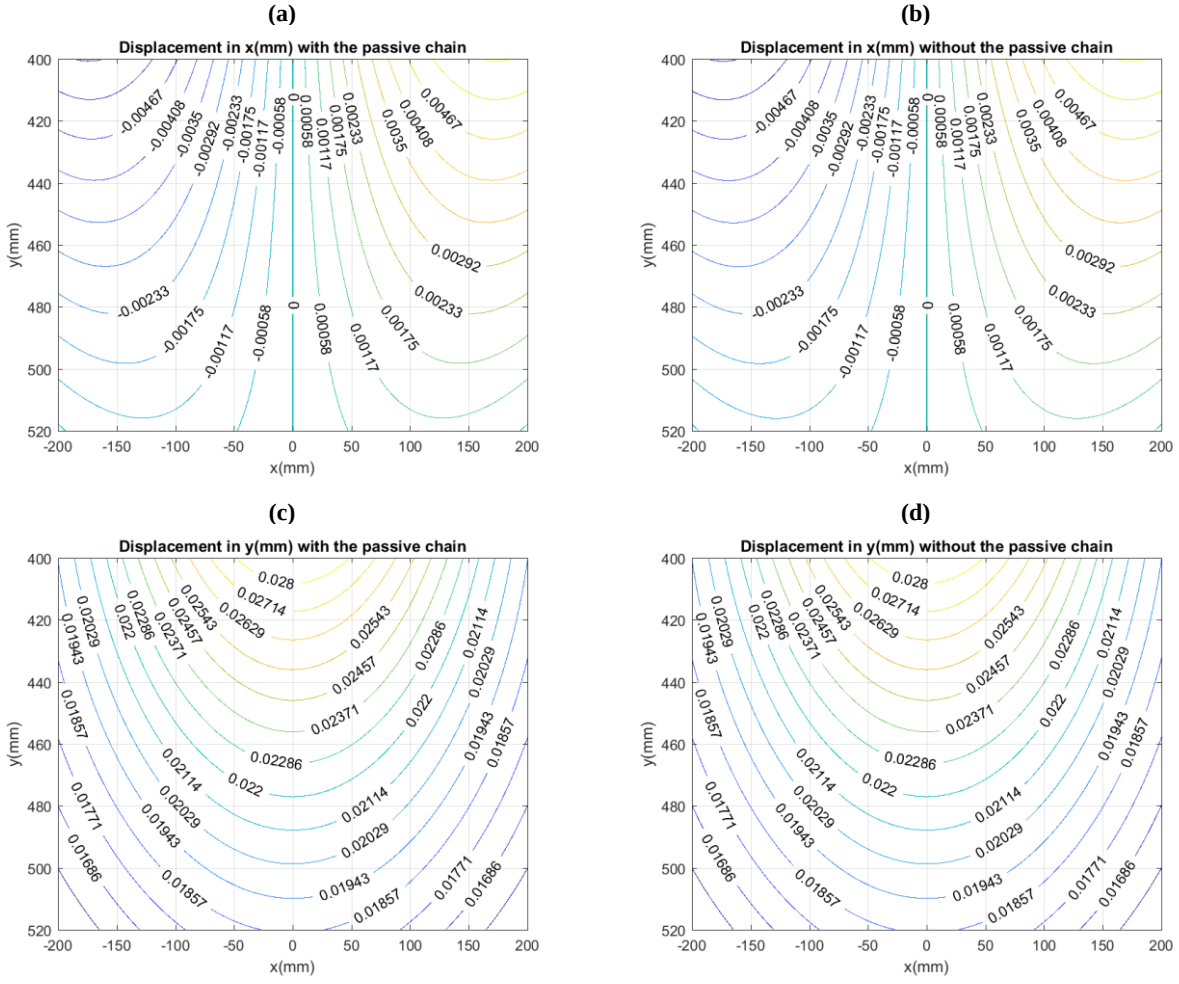

Figure 4 – Mapping of the workspace for displacement in x and y of the end effector modeled with the passive chain (a), (c) and without the passive chain (b), (d).

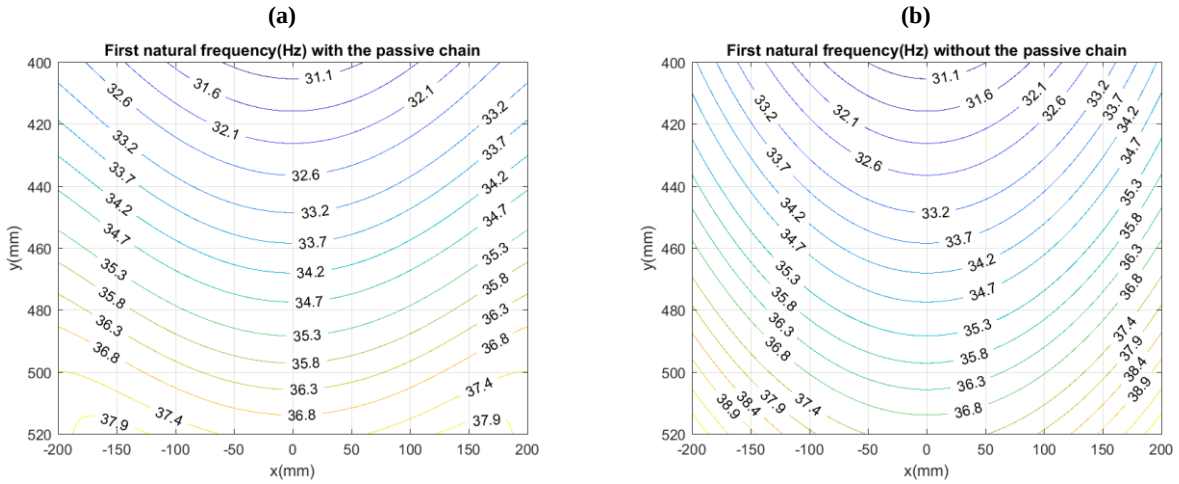

Figure 5 – Mapping of the workspace for the first natural frequency modeled with the passive chain (a) and without the passive chain (b).

4. CONCLUSIONS

Considering the obtained results, they lead to conclude that the stiffness of the passive chain, considering only the stiffness of the links, has a great relevance in maintaining the orientation of the end effector. This was shown by the similarity in the displacements in Fig. 4. The same did not occur in the mapping of the first natural frequency. This is due to the increased inertial effects in the mechanism by including the passive chain, slightly reducing the value of frequency and the mapping throughout the workspace. However, some sources of flexibility, such as joints, may have a greater effect on the stiffness of the mechanism and thus may be the subject of further investigation.

Regarding the use of the of lumped parameters method, the results of the consideration of the virtual actuators in the mathematical model were satisfactory, revealing the consistency of the method and its lower computational cost, since the stiffness matrix obtained refers only to the end effector. With the process being repeated for each position of the end effector along the workspace, other methods of analysis, such as the finite element method, become less suitable to mapping characteristics of the manipulator, since it is necessary to undo and redo the mesh of the model at each new configuration.

5. ACKNOWLEDGMENTS

Rodrigo Magalhães Cruz Alves Silva acknowledges grant 133844/2018-8, Conselho Nacional de Desenvolvimento Científico e Tecnológico (CNPq).

Fernando Malvezzi and Tarcisio Antonio Hess Coelho acknowledge grant #2018/12087-7, São Paulo Research Foundation (FAPESP).

6. REFERENCES

ABB Robotics, 2013, “IRB 360 FlexPicker ROB0082EN_F”, http://new.abb.com/products/robotics/industrial-robots/irb-360.

Adept Technology, 2010, “Adept Quattro s650H 09366-004 Rev. E”, http://www.adept.com/products/robots /parallel/quattro-s650h/downloads.

Bonev, I., 2019, “ParalleMIC – the Parallel Mechanisms Information Center”, http://parallemic.org/Terminology/ General.html. Accessed 10 July 2019.

Cammarata, A., 2016, “Unified Formulation for the Stiffness Analysis of Spatial Mechanisms”, Mechanism and Machine Theory, 105, 272-284.

Chablat, D., Wenger, P., 2003, “Architecture Optimization of the Orthoglide, a 3-DOF Parallel Mechanism for Machining Applications”, IEEE Transactions on Robotics and Automation, vol. 19, no. 3, pp 403-410.

Chen, W., 2001, “Dynamic modeling of multi-link flexible robotic manipulators”, Computers and Structures 79: 183-195.

Craig, J. J., 2005, “Introduction to Robotics: Mechanics and Control”, Addison-Wesley series in electrical and computer engineering: control engineering. Pearson/Prentice Hall.

Fontes, J. V., da Silva, M. M., 2016. "On the dynamic performance of parallel kinematic manipulators with actuation and kinematic redundancies". Mechanism and Machine Theory, 103, 148-166.

Gosselin, C. M., 1990, "Stiffness Mapping for Parallel Manipulators", IEEE Transactions on Robotics and Automation, 6(3), 377-382.

Gosselin C. M., Zhang, D., 2002, "Stiffness Analysis of Parallel Mechanisms using a Lumped Model", Int. Journal of Robotics and Automation, vol. 17, no. 1, pp 17-27

Haftka, R. T., Gürdal, Z., 1992, "Elements of Structural Optimization", Dordrecht: Kluwer Academic Publishers.

Hess-Coelho, T. A., 2007, "An Alternative Procedure for Type Synthesis of Parallel Mechanisms", In Proceedings of 12th IFToMM WORLD CONGRESS, 2007, Besançon.

Liang, D., Song, Y,, Sun, T., Jin, X., 2017, "Rigid-flexible coupling dynamic modelling and investigation of a redundantly actuated parallel manipulator with multiple actuation modes", Journal of Sound and Vibration 403:129–151.

Liu, H., Huang, T., Chetwynd, D. G., & Kecskeméthy, A., 2017, "Stiffness Modeling of Parallel Mechanisms at Limb and Joint/Link Levels", IEEE Transactions on Robotics, 33(3), 734-741.

Long, W., Guofeng, W., Haitao, L., Tian, H., 2018, "An approach for elastodynamic modeling of hybrid robots based on substructure synthesis technique", Mechanism and Machine Theory, 123:124-136.

Majou, F., Gosselin, C. M., Wenger, P., & Chablat, D., 2007, "Parametric Stiffness Analysis of the Orthoglide", Mechanism and Machine Theory, 42(3), 296-311.

Rezaei, A., Akbarzadeh, A., Akbarzadeh-T, M., 2012, "An investigation on stiffness of a 3-PSP spatial parallel mechanism with flexible moving platform using invariant form", Mechanism and Machine Theory, 51:195–216.

Silva, R. M. C. A., Hess-Coelho, T. A., 2019, "Analysis of a parallel manipulator for determination of promising kinematic and dynamic parameters", In Proc. of the 18th DINAME, Mar 10-15, Buzios, RJ, Brazil.

Tsai, L. W., 1999, "Robot Analysis: The Mechanics of Serial and Parallel Manipulators", New York: John Wiley & Sons.

Wang, X., Mills, J. K., 2005, "FEM dynamic model for active vibration control of flexible linkages and its application to a planar parallel manipulator", Applied Acoustics, 66:1151–1161.

Zhang, D., 2009, "Parallel Robotic Machine Tools", Springer Science & Business Media.

Zhang, D., Gosselin, C. M., 2002, "Kinetostatic Modeling of Parallel Mechanisms with a Passive Constraining Leg and Revolute Actuators", Mechanism and Machine Theory 37, 599–617.

Zhang, Q., Zhang, X., 2015, "Dynamic analysis of planar 3-RRR flexible parallel robots under uniform temperature change", Journal of Sound and Vibration, 21(1):81–104.

Zhao, Y., 2013, "Dynamic Optimum Design of a Three Translational Degrees of Freedom Parallel Robot while Considering Anisotropic Property", Robotics and Computer-Integrated Manufacturing, 29(4), 100-112.

Zi, B., Ding, H., Wu, X., Kecskeméthy, A., 2014, "Error modelling and sensitivity analysis of a hybrid-driven based cable parallel manipulator", Precisision Engineering, 38(1):197-211.

7. RESPONSIBILITY NOTICE

The authors are the only responsible for the printed material included in this paper.